Water Research 250 (2024) 121020

Contents lists available at ScienceDirect

Water Research

journal homepage: www.elsevier.com/locate/watres

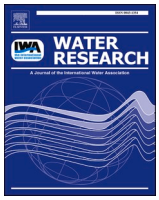

Breakdown of hardly degradable carbohydrates (lignocellulose) in a two-stage anaerobic digestion plant is favored in the main fermenter

Robert Heyer [a,b,c,#], Patrick Hellwig [a,d,#,*], Irena Maus [e,f], Daniel Walke [a,g], Andreas Schlüter [e], Julia Hassa [e], Alexander Sczyrba [e,f,h], Tom Tubbesing [e,h], Michael Klocke [i], Torsten Mächtig [j], Kay Schallert [b], Ingolf Seick [k], Udo Reichl [a,d], Dirk Benndorf [a,d,l]

[a] Otto von Guericke University, Bioprocess Engineering, Universitätsplatz 2, 39106 Magdeburg, Germany
[b] Multidimensional Omics Analyses Group, Leibniz-Institut für Analytische Wissenschaften – ISAS – e.V., Bunsen-Kirchhoff-Straße 11, 44139 Dortmund, Germany
[c] Multidimensional Omics Analyses Group, Faculty of Technology, Bielefeld University, Universitätsstraße 25, 33615 Bielefeld, Germany
[d] Bioprocess Engineering, Max Planck Institute for Dynamics of Complex Technical Systems, Sandtorstraße 1, 39106 Magdeburg, Germany
[e] Center for Biotechnology (CeBiTec), Bielefeld University, Genome Research of Industrial Microorganisms, Universitätsstraße 27, 33615 Bielefeld, Germany
[f] Research Center Jülich GmbH, Institute of Bio- and Geosciences (IBG), IBG-5: Computational Metagenomics, Leo-Brandt-Str., 52428 Jülich, Germany
[g] Otto von Guericke University, Database and Software Engineering, Universitätsplatz 2, 39106 Magdeburg, Germany
[h] Faculty of Technology, Bielefeld University, Universitätsstr. 25, 33615 Bielefeld, Germany
[i] Institute of Agricultural and Urban Ecological Projects affiliated to Berlin Humboldt University (IASP), Philippstraße 13, 10115 Berlin, Germany
[j] Christian-Albrechts-Universität Kiel, Institute of Agricultural Engineering, Olshausenstr. 40, 24098 Kiel, Germany
[k] Urban Water Management/Wastewater, Hochschule Magdeburg-Stendal, Breitscheidstrasse 2, 39114 Magdeburg, Germany
[l] Applied Biosciences and Process Engineering, Anhalt University of Applied Sciences, Microbiology, Bernburger Straße 55, 06354 Köthen, Germany

ARTICLE INFO

Keywords:
Biogas plant
Hydrolysis fermenter
Microbiome
Metaproteomics
Host-phage interactions
Multi-omics

ABSTRACT

The yield and productivity of biogas plants depend on the degradation performance of their microbiomes. The spatial separation of the anaerobic digestion (AD) process into a separate hydrolysis and a main fermenter should improve cultivation conditions of the microorganisms involved in the degradation of complex substrates like lignocellulosic biomass (LCB) and, thus, the performance of anaerobic digesters. However, relatively little is known about such two-stage processes. Here, we investigated the process performance of a two-stage agricultural AD over one year, focusing on chemical and technical process parameters and metagenome-centric metaproteomics.

Technical and chemical parameters indicated stable operation of the main fermenter but varying conditions for the open hydrolysis fermenter. Matching this, the microbiome in the hydrolysis fermenter has a higher dynamic than in the main fermenter. Metaproteomics-based microbiome analysis revealed a partial separation between early and common steps in carbohydrate degradation and primary fermentation in the hydrolysis fermenter but complex carbohydrate degradation, secondary fermentation, and methanogenesis in the main fermenter. Detailed metagenomics and metaproteomics characterization of the single metagenome-assembled genomes showed that the species focus on specific substrate niches and do not utilize their full genetic potential to degrade, for example, LCB.

Abbreviations: AD, Anaerobic digester/digestion; CAZymes, Carbohydrate-active enzymes; CID, Collision-induced dissociation; CSTR, Continuous stirred-tank reactor; DIET, Direct interspecies electron transfer; DSMZ, German Collection of Microorganisms and Cell Cultures; F, Main fermenter; GH, Glycoside hydrolase; GTDB, Genome Taxonomy Database; H, Hydrolysis fermenter; HRT, Hydraulic retention time; LCB, Lignocellulosic biomass; MAG, Metagenome-assembled genome; mgf, Mascot generic file; MG, MAG abundance based on normalized read abundance; MP, protein abundance, normalized; MPA, MetaProteomeAnalyzer; m/z, mass-to-charge ratio; OLR, Organic loading rate; PASEF, Parallel Accumulation Serial Fragmentation; READ, Single read abundance; SAOB, Syntrophic acetate-oxidizing Bacteria; SCFA, Short-chain fatty acids; TIMS, Trapped Ion Mobility Separation; t_{wm}, Tons wet mass; VFA, Volatile fatty acids.

* Corresponding author.
E-mail addresses: robert.heyer@isas.de (R. Heyer), hellwig@mpi-magdeburg.mpg.de (P. Hellwig), irena.maus@cebitec.uni-bielefeld.de (I. Maus), daniel.walke@ovgu.de (D. Walke), aschluet@cebitec.uni-bielefeld.de (A. Schlüter), jhassa@cebitec.uni-bielefeld.de (J. Hassa), asczyrba@cebitec.uni-bielefeld.de (A. Sczyrba), ttubbesing@uni-bielefeld.de (T. Tubbesing), mklocke@posteo.de (M. Klocke), tmaechtig@ilv.uni-kiel.de (T. Mächtig), kay.schallert@isas.de (K. Schallert), ingolf.seick@h2.de (I. Seick), ureichl@mpi-magdeburg.mpg.de (U. Reichl), benndorf@mpi-magdeburg.mpg.de (D. Benndorf).
shared first authors

https://doi.org/10.1016/j.watres.2023.121020
Received 23 June 2023; Received in revised form 5 December 2023; Accepted 13 December 2023
Available online 17 December 2023

Overall, it seems that a separation of AD in a hydrolysis and a main fermenter does not improve the cleavage of complex substrates but significantly improves the overall process performance. In contrast, the remaining methanogenic activity in the hydrolysis fermenter may cause methane losses.

1. Background

Lignocellulosic biomass (LCB) is a highly valuable renewable carbon source and energy carrier. For material and energetic utilization of LCB, numerous bioconversion technologies and biorefinery concepts were developed, aiming to establish a circular bioeconomy (review: Ubando et al., 2020). In this context, the anaerobic digestion (AD) of agricultural (by-) products and residues to biogas with methane and/or molecular hydrogen as an energetic component offers an unexploited potential for bioenergy production and reduction of greenhouse gas emissions (review: Dar et al., 2021).

In LCB, carbon is fixed in long-chained carbohydrates such as cellulose, hemicellulose, and xylan. In addition, certain biomasses can contain considerable amounts of proteins and, in minor amounts, lipids, both valuable substrates for bioconversion (review: e.g., Ling et al., 2022). In anaerobic environments, the decomposition of long-chained molecules proceeds in different phases (review: Cremonez et al., 2021). First, high molecular weight compounds are hydrolyzed in hydrolysis into soluble molecules, such as oligosaccharides, fatty acids, and amino acids. In the acidogenesis phase as the second step, these low molecular weight substances are converted preferentially to volatile fatty acids (VFA), namely acetic, propionic, and lactic acid, among others, with a production of gases, mainly carbon dioxide (CO_2) and molecular hydrogen (H_2). In the acetogenesis phase, VFAs are converted to acetic acid. Finally, in the methanogenesis phase, methane (CH_4) is formed either from CO_2 and H_2 (hydrogenotrophic methanogenesis) or from acetate (acetotrophic or acetoclastic methanogenesis).

The different degradation phases in AD are performed by the metabolic activity of a broad range of microbial species of both Bacteria and Archaea (e.g., Maus et al., 2016; 2017, 2020a). As early as 1971, the different growth optima of acidogenic bacterial species and methanogenic archaeal species were recognized, leading to the proposal of phase separation in AD by the introduction of a first fermentation stage with optimal growth conditions for “acid formers”, and a second fermentation stage optimized for “methane formers” (Pohland and Ghosh 1971). Today, agricultural resp. industrial two- (or more) stage two-phase AD reactor systems are typically operated with a first hydrolysis/acidogenesis fermenter featuring pH-values between 5.0 and 6.0 and hydraulic retention time (HRT) between 2 and 4 days for substrates, e.g., LCB as a sole substrate or in co-digestion with livestock manure, and, in series, a second methanogenesis fermenter with pH-values between 6.0 and 8.0 and HRT of 8 to 10 days (Cremonez et al., 2021).

The advantages and limitations of such two-stage phase-separated reactor systems for AD of LCB were discussed earlier (e.g., Schönberg and Linke 2012). However, all these studies were predominantly engineering-driven, focussing on fermenter design and operation, namely on pH control, substrate composition and organic loading rate (OLR), and corresponding chemical oxygen demand (COD) removal, VFA production, and CH_4-productivity resp. -yield. Surprisingly, the central hypothesis leading to the concept of AD phase separation, whether the metabolic activity of hydrolytic/cellulolytic/acidogenic bacteria is promoted by the conditions prevailing in the first hydrolysis/acidogenesis fermenter has surprisingly not been answered comprehensively for industrial-scale biogas reactors (Menzel et al., 2020).

Biogas-producing AD microbiomes are highly complex. Applying comprehensive metagenome data analysis, Campanaro et al. (2020) inventoried biogas microbiomes, leading to the compilation of metagenome-assembled genomes (MAGs) for more than 1600 species from AD systems. However, only a very limited number of these species, i.e., less than 5 %, were assignable to physiologically characterized species (Campanaro et al., 2020). In engineered AD systems, varying fractions of these species are detectable; major fractions of the microbial AD communities could not be classified down to the species level (‘microbial dark matter’).

Comprehensive genome-centered metagenomics analysis enables the unraveling of AD microbial dark matter and allows prediction about its functionality (Hassa et al., 2018). In addition, metagenome sequence data provides exclusive information on the presence of resp. abundance of microbial species, as well as an overview of their genetic potential.

Contrary, it must be noted that the occurrence of a certain microbial species with particular metabolic features does not necessarily imply its metabolic activity and substantial participation in AD.

To distinguish between the metabolically active and inactive parts of the AD microbiome members, combined metagenomics and metaproteomics analysis supported by integrated bioinformatic data analysis is advantageous (integrated or multi- resp. poly-omics) (Heyer et al., 2019a). Unfortunately, comprehensive, integrated omics studies on the impact of alteration of AD process factors resp. technical improvements in AD on the inherent microbiome’s functionality with a reliable statistical background are still very limited (e.g., Abendroth et al., 2017).

To overcome this lack aiming to answer the unsolved question of the eligibility of a hydrolysis stage to support the LCB breakdown, an integrated poly-omics approach was applied focusing on the following questions: (i) What are the structural and functional differences between the specialized AD microbiomes present in the hydrolysis/cellulolytic stage and the methanogenesis stage? (ii) How stable is the structure and functionality of the specialized AD microbiomes during one year of continuous operation?

2. Material and methods

In the following, the methods used are described in brief. For more details, refer to Supplementary Note.

2.1. Description of the anaerobic digester and sampling

The sampled two-stage anaerobic digester system consists of one not gas-tight, continuous stirred tank reactor (CSTR) for hydrolysis (H) with a volume of 180 m^3, one main CSTR for biomethanation (F) with a volume of 2000 m^3 and one secondary fermenter (1030 m^3) (Supplementary Figure 2). On average, the daily substrate feeding into H was 77.3 tons wet mass (t_{wm}) ± 5.0 t_{wm}. It consisted of 11.3 m^3 ± 0.5 m^3 liquid pig manure, 1.4 m^3 ± 0.6 m^3 liquid silage effluent, 0.3 t_{wm} ± 0.3 t_{wm} corn-cob-mix, 13.3 t_{wm} ± 1.6 t_{wm} maize whole crop silage, 0.2 t_{wm} ± 0.3 t_{wm} solid fermentation residues, and 1.5 t_{wm} ± 1.8 t_{wm} seasonal (from October 2016 to March 2017) beet silage. Additionally, the daily substrate feeding was mixed with 49.2 m^3 ± 4.6 m^3 liquid fermentation residues from the subsequent secondary fermenter. This substrate supply corresponded to an organic loading rate (OLR) of 40.0 $kg_{VS}\ m^{-3}\ d^{-1}$ ± 4.3 $kg_{VS}\ m^{-3}\ d^{-1}$ for H and 3.2 $kg_{VS}\ m^{-3}\ d^{-1}$ ± 0.5 $kg_{VS}\ m^{-3}\ d^{-1}$ for F, respectively, at a hydraulic retention time (HRT) of 2.3 d ± 0.2 d for H and 25.7 d ± 1.7 d for F. The process temperature in F was 39.7 °C ± 0.2 °C. In contrast, process temperature in H was measured only exemplarily, while the measurements of nine-time points were about 39.9 °C ± 1.2 °C.

H and F were sampled monthly from November 2016 to October 2017 (H1-H12, F1-F12). The samples were stored at −21 °C until further use. Furthermore, the operation data of the biogas plant were collected for the entire year (Supplementary Note A1.).

2.2. Taxonomic and functional microbiome characterization

One metagenome for timepoint T4 for the hydrolysis and one for the main fermenter was created as described previously (Maus et al., 2020b) with an Illumina HiSeq sequencer using the Illumina HiSeq Rapid SBS kit v2 (500 cycles) in a 2 × 250 bp paired-end run. Functional classification of the genes, including KEGG pathway mapping, was performed with the Diamond tool (Buchfink et al., 2015). Subsequently, metagenome-assembled genomes (MAGs) were computed with MetaBAT (v0.21.3) (Kang et al., 2019), and the Genome Taxonomy Database toolkit (GTDB) taxonomy was assigned (Chaumeil et al., 2019).

Metaproteomics analysis was carried out according to Heyer et al. (2019b) using phenol extraction into a ball mill, FASP digestion, and LC-MS/MS using an UltiMate® 3000 nano splitless reversed-phase nanoHPLC (Thermo Fisher Scientific, Dreieich) coupled online to a timsTOF™ pro mass spectrometer (Bruker Daltonik GmbH, Bremen).

For the functional characterization of the identified genes, proteins, and MAGs, the sequenced genes were assigned to metabolic pathways, functions, and carbohydrate-active enzymes (CAZymes) using the MPA_Pathway_Tool (http://141.44.141.132:9001/home) (Walke et al., 2021), which provided already a comprehensive set of 49 pathways relevant for the AD process based on Sikora et al. (2019) and Heyer et al. (2019b). Furthermore, we created with the MPA_Pathway_Tool CAZy profiles for H and F using the EC numbers in the gene table mapped to Glycoside hydrolase (GH) families from the CAZy database (http://www.cazy.org/, retrieved on 20.12.2022, http://www.cazy.org/Glycoside-Hydrolases.html, Drula et al. (2022)).

2.3. Integrative analysis of metagenomics and metaproteomics data

Metagenomics and metaproteomics data were integrated by in-house scripts developed in JAVA (version 1.8, Supplement jarZIP). In the first step, the list of all genes was enriched by the matching MAG_ID. Second, the gene abundance for H and F was added based on the total read count of the MAG (or contigs, which were not assembled to MAG) normalized by the MAG length. Third, the protein spectral abundance was added using the peptide identification files once for all peptides and once only for unique peptides. The spectral abundance of peptide identifications (Drula et al., 2022) assigned to multiple proteins was distributed equally to all associated proteins. In the fourth step, based on the normalized read and spectral counts, we created an abundance profile for the MAGs. For comparison, the abundance profiles were normalized to 100 % for each sample.

2.4. Replicates, statistics evaluation, and visualization

In this study, twelve samples of H and F of an anaerobic digestion plant were analyzed for one year (Nov-16 - Nov-17) with metaproteomics and for timepoint T4 with metagenomics. Metaproteomics and -genomics analysis were carried out in triplicates. R-Statistics version (1.2.5001) was used for statistical analysis. The Shapiro test validated normal distribution for comparing protein abundance between H and F. Although this criterion was not fulfilled for low abundant proteins, we used a *t*-test combined with Benjamini-Hochberg correction (p-value < 0.05) instead of a Mann-Whitney U-Test. Clustered heatmaps were created based on metaproteomics- and -genomics data using the "ComplexHeatmap" library (Gu et al., 2016).

3. Results

3.1. Technical and chemical process parameters

Feeding of 77.3 ± 5.0 tons substrate (mainly maize silage, pig manure, and seasonal beet silage) per day revealed a stable biogas production over the entire evaluation period of 2883.0 ± 283.9 m^3 per day (average 60.2 ± 1.5% methane in F, Fig. 1 and Supplementary

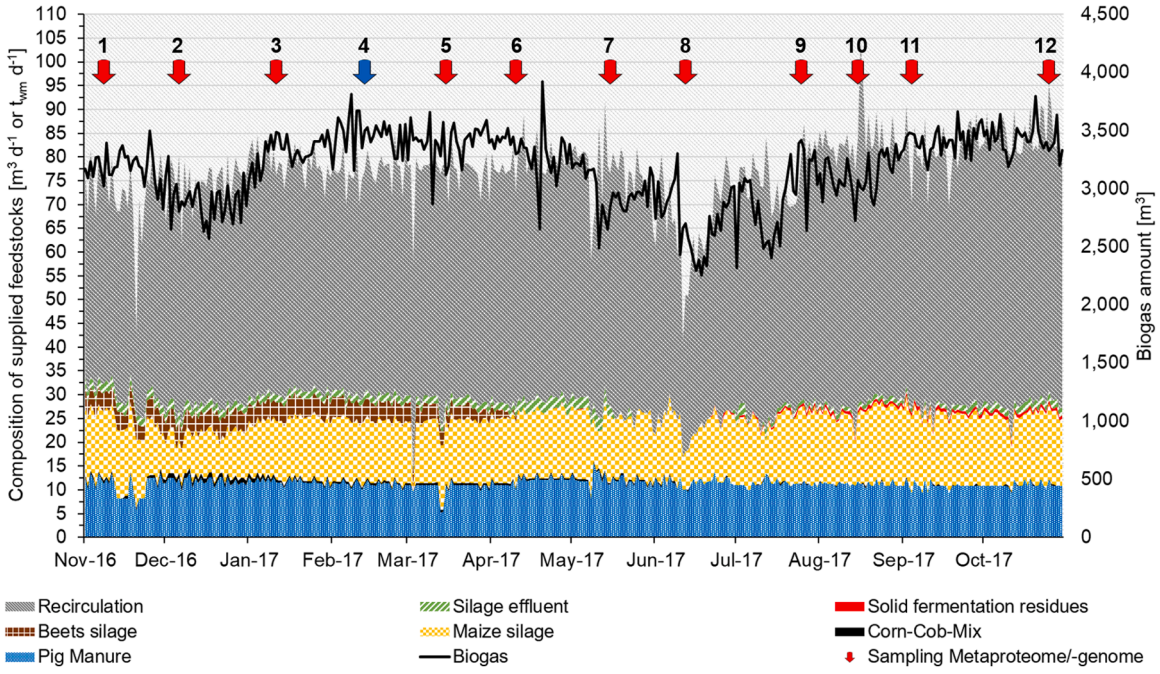

Fig. 1. Time course of feeding and biogas production over one year. Sampling for metaproteomics was carried out monthly (red arrows) from 08.11.2016 to 25.10.2017 for the hydrolysis fermenter (H1-H12) and main fermenter (F1-F12) (Supplementary Table 1). The blue arrow indicates the time point (4) of sampling for metagenome sequencing (H04/F04, 13.02.2017). This time point was selected due to the stable biogas production and feeding conditions (wide variety of substrates). The feeding of the biogas plant consisted of recirculation from a secondary fermenter [$m^3\ d^{-1}$]), silage effluent [$m^3\ d^{-1}$], solid fermentation residues [$t_{wm}\ d^{-1}$], beets silage [$t_{wm}\ d^{-1}$], maize silage [$t_{wm}\ d^{-1}$], corn-cob mix [$t_{wm}\ d^{-1}$] and pig manure. The black line indicates the biogas production as measured daily at the combined heat and power plants. The methane content of the plant was 60.2 vol.% ± 1.5 vol.%. The full data set is shown in Supplementary Table 1. (For interpretation of the references to colour in this figure legend, the reader is referred to the web version of this article.)

Table 1). The composition of the substrate remained almost stable, except for adding small amounts of seasonal substrates such as beet silage or corn-cop mix (<2.0 % of the feed). Comparisons of the average process parameters between H and F revealed different conditions in H and F regarding retention times (HRT_F: 25.7 days / HRT_H: 2.3 days, p-value < 3.69×10^{-13}), pH (pH_F: 7.9 / pH_H: 5.9, p-value: 2.04×10^{-9}) and total short-chain fatty acid (SCFA) concentrations ($SCFAs_F$: 118.7 mg L^{-1}/ $SCFAs_H$: 14,378.0 mg L^{-1}, p-value: < 1.12×10^{-10}) (Supplementary Table 2). Furthermore, we observed a shift in the SCFA composition between both fermenters (e.g., butyrate was only present in H, Fig. 2).

3.2. Microbiome's taxonomic and functional profile deduced from metagenome and metaproteome data analysis

Metagenome analysis of triplicated samples from H and F (sampling timepoints F4, H4, Fig. 1) revealed 124,228,795 reads leading to the assembly of 1,034,301 genes with a subsequent compilation of 262 MAGs (Supplementary Table 3) resp. 49 of high quality (>90 % completeness, <5 % contamination) (Bowers et al., 2017) (Fig. 4, Supplementary Table 4). Metaproteomics analysis with protein identification against the deduced protein sequences from the metagenome resulted overall in 2,193,991 identified spectra and 55,487 identified proteins (Supplementary Table 5). This corresponds to an average of 30, 472 ± 8,122 identified spectra and 14,026 ± 2,788 proteins per measurement. Subsequently, the microbiome's detailed taxonomic and functional composition was evaluated, as shown in Supplementary Note C1, and the microbial key players were summarized in Fig. 3. Furthermore, we included a detailed characterization of phage proteins in Supplementary Note D and of all other proteins in Supplementary Note C.

3.3. Differentially abundant taxa in hydrolysis and main fermenter

3.3.1. Abundance of MAGs

A systematic comparison of the MAG abundances between H and F revealed in total of 40 resp. 29 MAGs of 49 high abundant MAGs with significantly altered abundance values in the metagenome or metaproteome data (p-value below 0.05 with Benjamini-Hochberg correction). Thereby, metaproteomics and metagenomics data revealed comparable ratios between the MAG abundances in H and F (the same trend means ratio H vs. F was either above or below 1). For example, MAG_119 (genus *Eubacterium_H*, $ratioMG_{H/F}$: 26.4, $ratioMP_{H/F}$: 28.3) and MAG_223 (genus *Olsenella_B*, $ratioMG_{H/F}$: 16.5, $ratioMP_{H/F}$: 23.5) were more abundant in H and MAG_2 (genus *Methanothrix*, $ratioMG_{H/F}$: 0.3, $ratioMP_{H/F}$: 0.3) and MAG_226 (family *4484–276*, $ratioMG_{H/F}$: 0.0, $ratioMP_{H/F}$: 0.4) more in F.

Exceptions from the similar trends between metagenomics and metaproteomics data were observed for MAG_69 (species: *Herbinix luporum*, $ratioMG_{H/F}$: 1.6, $ratioMP_{H/F}$: 0.8) and four other MAGs with low abundance in metaproteomics data: MAG_255 (genus *UBA2730*, $ratioMG_{H/F}$: 78.2, $ratioMP_{H/F}$: 0.9), MAG_183 (genus UBA5266, $ratioMG_{H/F}$: 0.1, $ratioMP_{H/F}$: 1.7), MAG_21 (genus *Eubacterium_B*, $ratioMG_{H/F}$: 40.5, $ratioMP_{H/F}$: 0.6), and MAG_187 (genus UBA1046, $ratioMG_{H/F}$: 0.2, $ratioMP_{H/F}$: 1.8). MAG_255 exhibits high abundances in H on the metagenome level (13.68%) but much lower abundances in the metaproteome (0.06%), indicating the presence of spores.

3.3.2. Predicted metabolic pathways in hydrolysis and main fermenter

Comparison of the degradation performance based on protein abundances assigned to main metabolic functions (Fig. 4) between H and F showed that based on metaproteome data analysis complex polysaccharides e.g., cellulose ($ratioMG_{H/F}$: 0.92, $ratioMP_{H/F}$: 0.46), aromats ($ratioMG_{H/F}$: 0.09, $ratioMP_{H/F}$: 0.14, $p > 0.05$), fatty acids ($ratioMG_{H/F}$: 0.52, $ratioMP_{H/F}$: 0.64), and proteins ($ratioMG_{H/F}$: 0.82, $ratioMP_{H/F}$: 0.53, $p > 0.05$) are mainly degraded in F. In contrast, the degradation of starch ($ratioMG_{H/F}$: 1.22, $ratioMP_{H/F}$: 10.95, $p > 0.05$), other sugars ($ratioMG_{H/F}$: 0.58, $ratioMP_{H/F}$: 2.73, $p > 0.05$), and hemicellulose ($ratioMG_{H/F}$: 0.66, $ratioMP_{H/F}$: 2.04) were elevated in H. This trend was only observed in metaproteomics data, indicating that the microorganisms have the genetic potential but adjust their enzyme expression profiles.

Enzymes for primary fermentation to ethanol ($ratioMG_{H/F}$: 1.51, $ratioMP_{H/F}$: 1.09), acetate ($ratioMG_{H/F}$: 0.97, $ratioMP_{H/F}$: 1.71, $p > 0.05$), and lactate ($ratioMG_{H/F}$: 4.57, $ratioMP_{H/F}$: 26.72, $p > 0.05$) were observed in higher abundance in H. Increased abundance of the Wood-Ljungdahl-pathway ($ratioMG_{H/F}$: 0.70, $ratioMP_{H/F}$: 0.39), formiate fermentation ($ratioMG_{H/F}$: 0.54, $ratioMP_{H/F}$: 0.24) and hydrogenases proteins ($ratioMG_{H/F}$: 0.17, $ratioMP_{H/F}$: 0.36) indicated enhanced

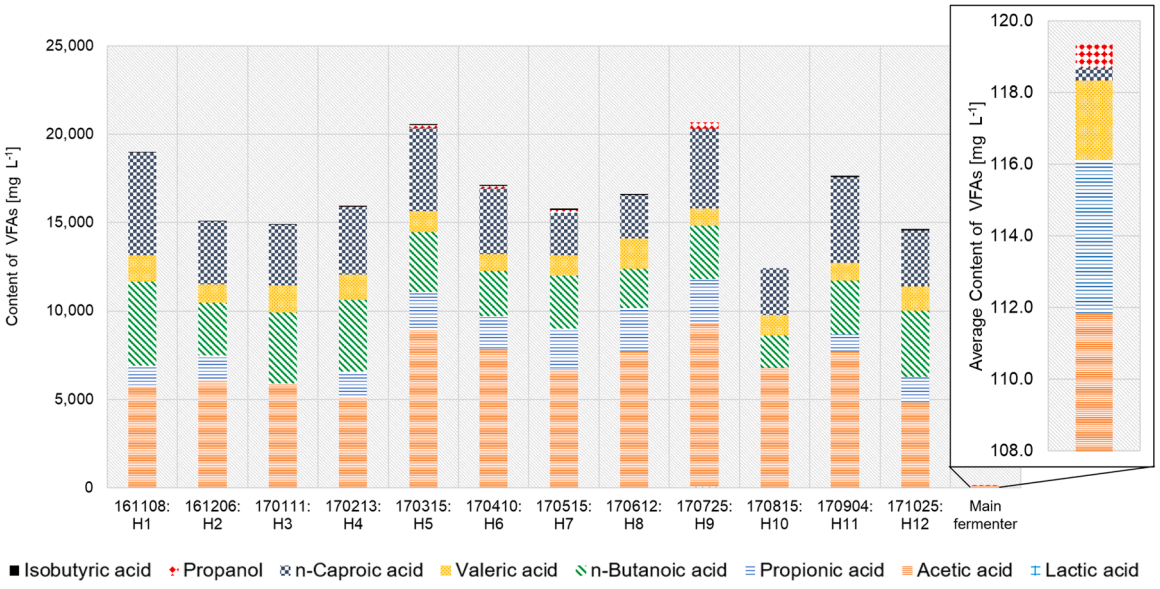

Fig. 2. Short-chain fatty acids from samples of the hydrolysis and main fermenter. The content of detected volatile fatty acids (VFAs) was determined by high-performance liquid chromatography analysis as described by Jan Liebetrau, Diana Pfeiffer, and Daniela Thrän (2015). The bar on the right section shows the average VFA concentration in the main fermenter (F), which was at least 100-fold lower than in the hydrolysis fermenter (H). The full data set is shown in Supplementary Table 1.

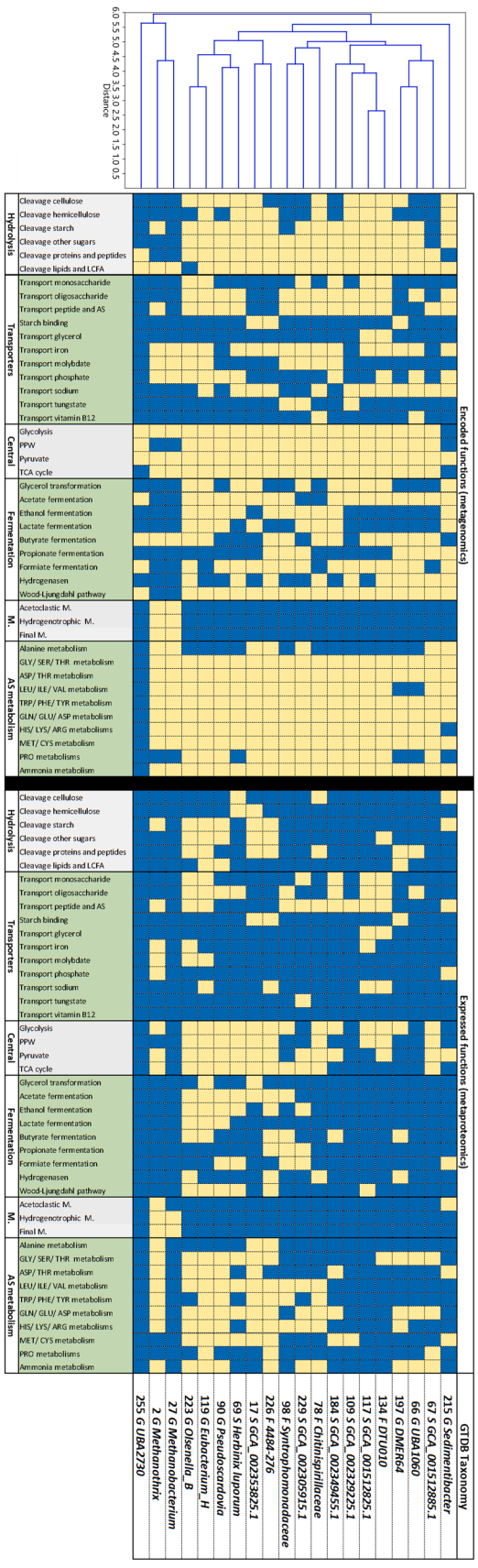

(caption on next column)

Fig. 3. Metabolic potential and expressed functions of high-abundant and high-quality metagenome-assembled genomes (MAGs). The abundance of high-quality MAGs (completeness > 90 %, error rate < 5 %) in hydrolysis or main fermenter was deduced from metagenome or metaproteome data above 1 % to the main metabolic functions. The yellow color indicates the presence, and the blue indicates the absence of the function within the metagenome and metaproteome of the MAG. Additionally, the data were clustered based on the metagenome data using UPGMA and "Euclidean" distance. Abbreviations: M (methanogenesis), AS (amino acids). Most precise taxonomic information for numeric GTDB taxonomies: MAG 67 (o_Bacteroidales), MAG 66 (g_Syntrophosphaera), MAG 197 (o_Bacteroidales), MAG 134 (f_Peptococcaceae), MAG 117 (c_Limnochordia), MAG 109 (f_Acutalibacteraceae), MAG 184 (f_Lachnospiraceae), MAG 229 (f_Pelotomaculaceae), MAG 226 (o_Bacteroidales), MAG 17 (g_Prevotella), MAG 255 (c_Bacilli). (For interpretation of the references to colour in this figure legend, the reader is referred to the web version of this article.)

secondary fermentation in F (Fig. 4). Furthermore, acetoclastic methanogenesis (ratioMG$_{H/F}$: 0.51, ratioMP$_{H/F}$: 0.39, $p > 0.05$), hydrogenotrophic (ratioMG$_{H/F}$: 1.25, ratioMP$_{H/F}$: 0.41, $p > 0.05$) and the final step of the methanogenesis (ratioMG$_{H/F}$: 0.88, ratioMP$_{H/F}$: 0.36, $p > 0.05$, EC 2.1.1.86, EC 2.8.4.1, EC 1.8.98.1) were also more abundant in F.

3.3.3. Diversity of microbial carbohydrate-active enzymes in the hydrolysis and main fermenters encoded in abundant metagenome-assembled genomes

Due to enriched sugar consumption in H, CAZymes relevant to the AD process were analyzed in detail, focussing on the glycoside hydrolase families (GH) for (i) endo- and exo-1,4-β-d-glucanases (cellulases), (ii) starch and glycogen hydrolases, (iii) lysozymes and chitinases (cell wall degradation), (iv) oligosaccharide phosphorylases, (v) glycosidases (hydrolysis of single sugar residues from non-reducing ends), and (vi) hemicellulases (Fig. 5, Supplementary Table 8).

Whereas MG data confirmed a wide potential for the degradation of carbohydrates, evidence for the expression of corresponding enzymes was partially missing. Nearly all GH families were present for the degradation of (i) cellulose, (ii) starch and glycogen, and (v) single sugar residues, while roughly half of the GH families for the degradation of (ii) hemicellulose (6 of 11 missing), and (vi) oligosaccharides (1 of 2) were missing in MP data. No enzymes were identified for the degradation (iv) of cell wall components (Fig. 5).

Except for GH11 (xylanase) and GH78 (rhamnosidase), MG and MP data indicated similar abundances of GH families in H and F. Overall, 20 of 46 GH families were more abundant in F and 11 more in H. The GH families enriched in H focused on easily degradable carbohydrates such as the degradation of starch by GH13, xylane by GH,11, and maltose by GH4. In F, nearly all GH families for complex carbohydrate degradation, such as cellulases and hemicellulases, were enriched (Fig. 5i and vi).

3.4. Metaproteomics analysis of annual dynamics of the microbiomes in H and F based on MP

In addition to comparing H and F for time point four, the annual dynamic of all MAGs (Supplementary Table 10) and the metabolic functions (Supplementary Table 11) were analyzed to assess the stability of the microbiome. Based on the average Spearman correlation factor of 0.99 for the MAGs and 0.97 for the metabolic functions, the microbiome in F was more similar across the different time points than in H with 0.91 vs. 0.95 (Supplementary Note C5.). Furthermore, the correlation analysis of all MAGs and of the main metabolic functions showed that the samples from the first four time points of H were different compared to the other time points.

In contrast to the high correlation between entire MAG profiles of all time points, greater variations in the abundance of the single MAGs were observed, as indicated by an average MAG standard deviation of 90 % in H and 92 % in F (based on the standard deviation divided by MAG

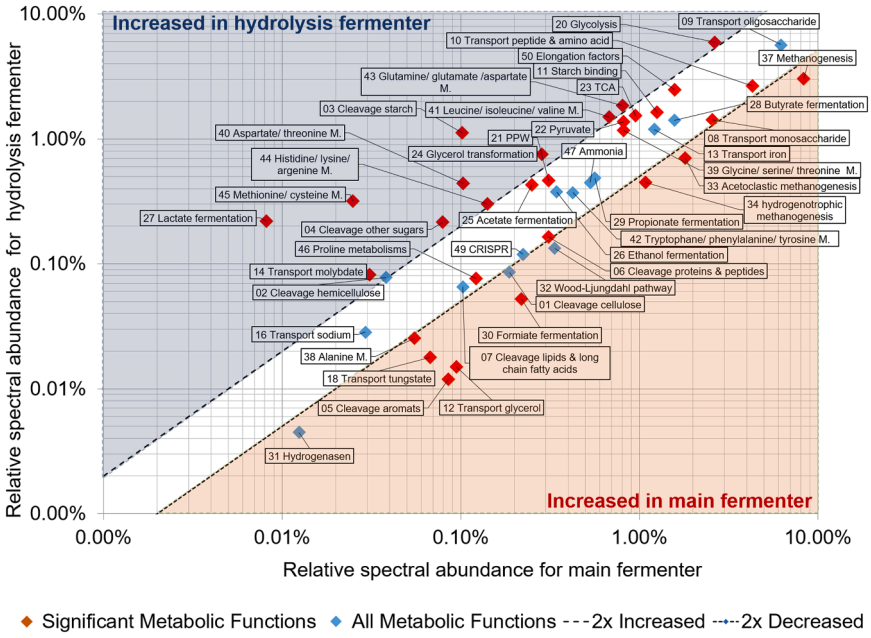

Fig. 4. Overview of the main metabolic functions enriched in the hydrolysis (H) and main fermenter (F) based on metaproteome data. The blue rhombus represents the metabolic function. Significant changes (*t*-test, p-value after Benjamini-Hochberg correction < 0.05) are highlighted in red. The blue area indicates a 2-fold increase in the H, and the orange area indicates a 2-fold increase in F of the metabolic function. The spectra were normalized to 100 %. The data can be found in Supplementary Table 7. (For interpretation of the references to colour in this figure legend, the reader is referred to the web version of this article.)

abundance). Also noteworthy were the expression profiles of certain metabolic functions, such as cellulose degradation (Fig. 6). In general, proteins for cellulose degradation were more abundant in F, with an even much higher abundance for timepoint ten.

To assess whether the single MAGs focus on certain substrates, we performed, in addition to the functional analysis, Spearman correlation analysis ($|R|>0.75$) between the metaproteome-based MAG abundance and the substrates (Supplementary Table 12). Furthermore, we included organic loading rate, hydraulic retention time, pH value, and total nitrogen ammonia (TAN) in the correlation analysis to check for niche preference. We observed 25 (exclusive self-correlations) correlations in H and 22 in F. A high positive correlation for H and F could be observed between the MAG_223 (genus *Olsenella_B*) and the amount of fed sugar beets and corn-cop mix, as well as a negative correlation for the amount of maize silage. Furthermore, MAG_119 (genus *Eubacterium_H*) in F correlated with the amount of sugar beet. The corn-cop mix was positively correlated in H with MAG_184 (family *Lachnospiraceae*) and F with MAG_134 (family *Peptococcaceae*).

Silage effluent had a strong negative impact on MAG_67 (order *Bacteroidales*) in F. Within the acid spectrum, we could only identify a high negative correlation between the amount of n-butanoic acid and the MAG_67 (species *Herbinix luporum*) in H. Furthermore, we observed several positive correlations between the fermenting MAGs, such as between MAG_69 (genus *Herbinix luporum*) and MAG_197 (family *Rikenellaceae*) in H or MAG_215 (G *Sedimentibacter)* and MAG_98 (F *Syntrophomonadaceae*) in F.

4. Discussion

Compared to single-stage AD reactors, two-stage phase-separated fermenter systems have shown several advantages in laboratory-scaled LCB fermentation experiments, namely higher overall methane yields (Pakarinen et al., 2009), higher methane concentrations in biogas (obtained from the methanogenesis stage) (Schönberg and Linke 2012), thus, enabling higher energy recovery (Shen et al., 2013). Additionally, two-phase digestion revealed more stable operation and higher OLR treatment capacity (Shen et al., 2013). On the other hand, some studies showed superior AD performance for two-stage systems only in the case of substrates with high sugar content (Lindner et al., 2016).

In general, the AD phase separation of the AD process is assumed to improve AD performance by preventing shock loads and improving viscosity by mixing with digestate (Menzel et al., 2020). AD reactor construction designs enable fermentation settings optimal for microbial growth (i.e., pH values) for hydrolytic and fermenting bacteria in H, acetogenic bacteria, and methanogenic archaea in F (Cheng Zhang and Noike 1991). However, up to now, little knowledge has been available about the impact of separated H and F on the AD microbiome and its performance (Menzel et al., 2020).

4.1. Operation of the anaerobic digester

Overall, the process parameters of the investigated AD, including the acid profile and biogas production, were stable over time and similar to other two-stage ADs (Menzel et al., 2020). However, compared to F, H showed a decreased pH value and more variations of the produced short-chain fatty acids, matching the reduced retention times and high organic loading rates. Beet silage was seasonally fed (November till May), which led to some fluctuations but did not influence the process significantly. Compared to one-stage ADs (usually 55 %), the methane concentration in the biogas was elevated in the investigated two-stage AD (60%), a possible explanation being that CO_2 is already produced and released in H. However, since H was not gas-tight and the biogas amount and composition were measured just for the complete biogas plant, assessing the biogas yield and productivity in H was not feasible. However, this information would enable a better understanding of the influence of H on the biogas production of this specific biogas plant.

4.2. High-resolution microbiome comparison of hydrolysis versus the main fermenter

Separation of the AD process in a small H and a large F resulted in partial separation of hydrolysis and acidogenesis in H from acetogenesis and methanogenesis in F. For example, the fermenting MAGs_119 (genus *Eubacterium_H*) and MAG_223 (genus *Olsenella_B*) and metabolic process

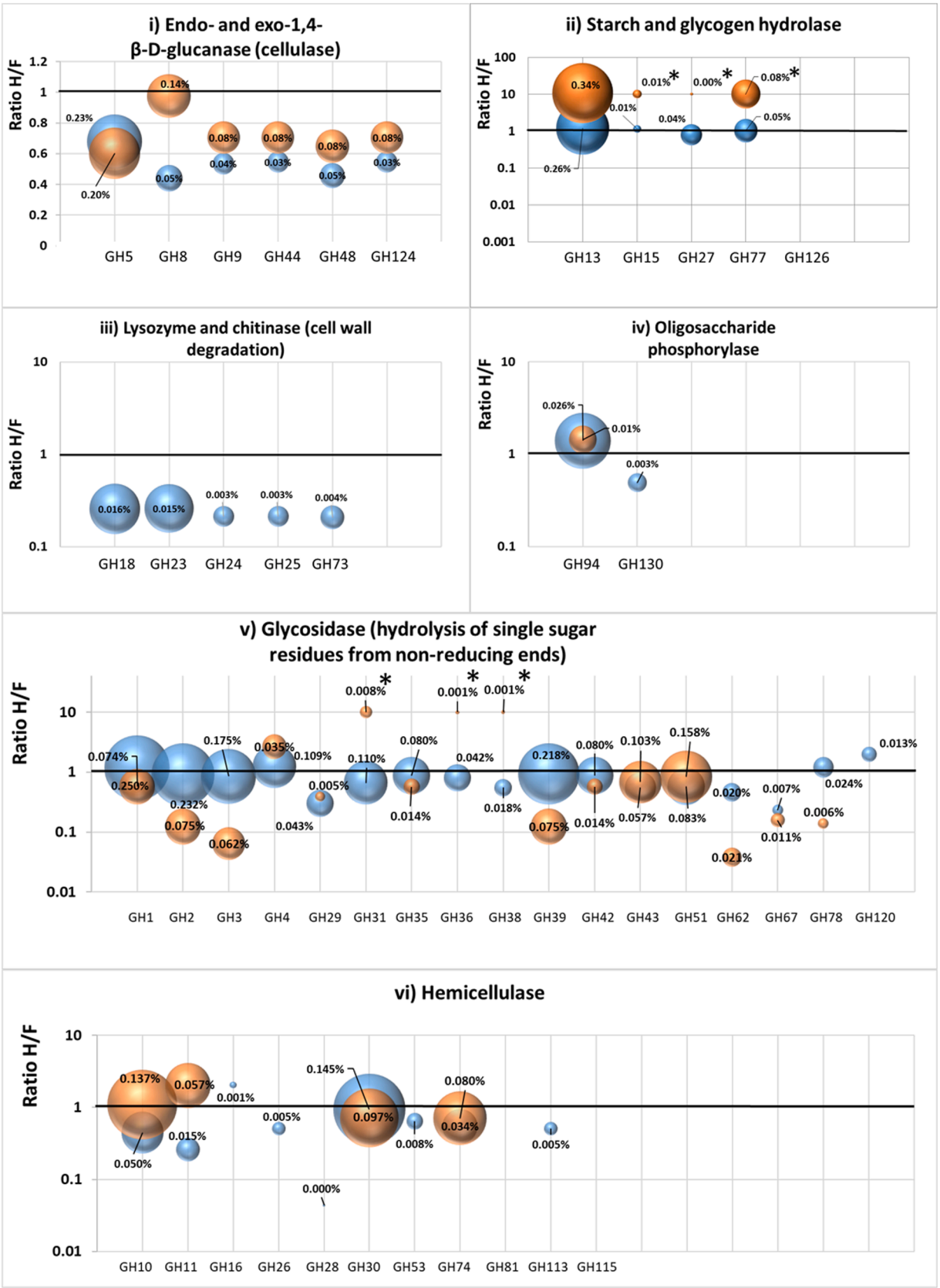

Fig. 5. Enrichment of CAZys in the hydrolysis (H) and the main fermenter (F) based on the relative abundance of samples analyzed by metaproteomics and -genomics. The bubbles represent the abundance in the metaproteomic (orange) and metagenomic (blue) data, respectively. The center point of the bubbles shows the ratio H to F. If proteins for the GH family were found only in the hydrolysis fermenter, the ratio was set either to "10″ and marked with a star. (For interpretation of the references to colour in this figure legend, the reader is referred to the web version of this article.)

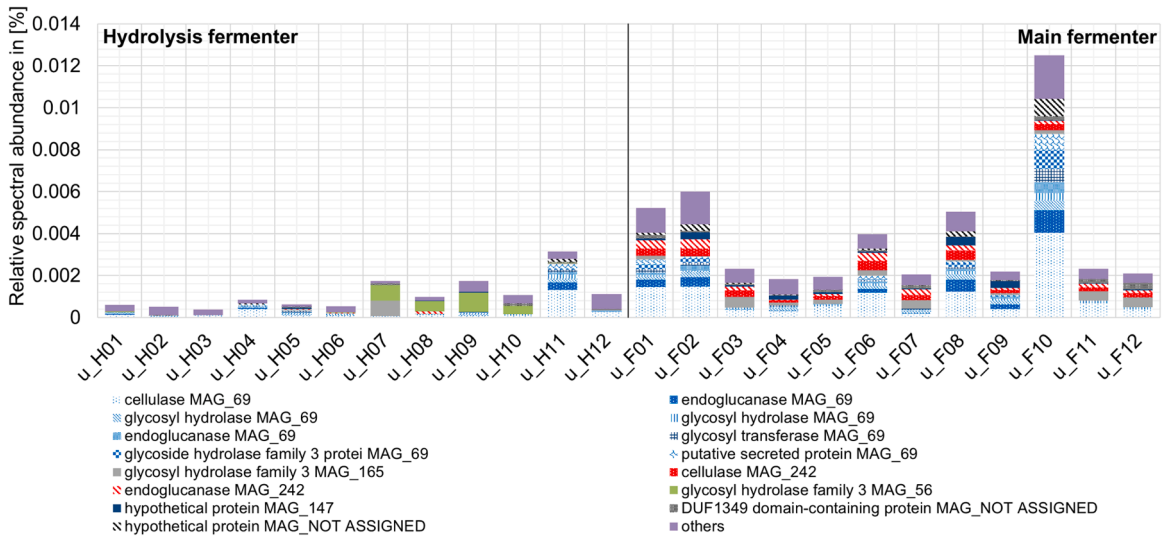

Fig. 6. All enzymes involved in cellulose degradation for the analyzed time period are based on the spectral abundance. The enzymes belonging to cellulose degradation were identified by their EC number. All information on the time points can be found in Fig. 5 and Supplementary Table 1. Low abundance enzymes below 100 spectra over all samples were agglomerated to "others". The data can be found in Supplementary Table 11.

cleavage of starch and lactate fermentation were more abundant in H. In contrast, proteins assigned to the function methanogenesis (MAG_2, genus Methanothrix) were increased in F.

At first glance, improved degradation of proteins and easy-degradable carbohydrates (i.e., starch, cellobiose, and maltose) in H confirmed the hypothesis that spatial separation providing optimal conditions for hydrolysis could enhance the anaerobic digestion process. In contrast, enzymes for the degradation of complex carbohydrates were more abundant in F, questioning the concept of spatial separation. Obviously, easily degradable substrates are metabolized first, enabling faster growth of the corresponding hydrolytic species. The faster growth was confirmed by a higher abundance of translational and cell cycle proteins in H with shorter retention times. The observed failure to transfer the hydrolysis of complex carbohydrates to H might explain, in retrospect, the rare application of spatial separation in full-scale AD plants in Germany and elsewhere (Schories et al., 2018). However, it should be noted that the analysis relied on the CAZy assignments, and there may be additional sugar-degrading enzymes may not be assigned.

Furthermore, the applied recirculation from the secondary fermenter to H causes a high abundance of methanogenesis genes and proteins (proteins for final methanogenesis >3 %). Therefore, it may indicate a loss of methane in open H. In the worst case, methane release decreases AD's profitability and promotes global warming. But considering the acidic pH in H and the partial influx of oxygen from feeding, high methane production in H is not expected. Nevertheless, since methane production was observed in similar cases, it should be monitored in future projects and full-scale plants with open H (Patel et al., 1990; Shimada et al., 2011).

The community structure revealed that about 20 MAGs, representing 50 % of the total abundance, dominated the AD microbiome (based on MG and MP). Among these 20 MAGs, Phyla *Firmicutes* was most abundant, which is also supported by other studies (e.g., Stolze et al., 2015). The *Archaea* community was dominated by *Methanothrix*.

Furthermore, several core functions such as cellulose cleavage (MAG_69, species *Herbinix luporum*) or methanogenesis (MAG_02, genus *Methanothrix*) were dominated by one taxon, indicating that the dominating MAGs found strategies to outcompete other species. Detailed knowledge about the key species could initiate the specification of taxa's functions in the microbial network of anaerobic digestion. In particular, the expression of all proteins for hydrogenotrophic methanogenesis in *Methanothrix* (MAG_2), formerly described to be strictly acetoclastic (Stams et al. 2019; Vrieze et al., 2012), points to strong syntrophic interactions using direct interspecies electron transfer (DIET). A better understanding of the key players and the metabolic interactions could be applied to improve the living conditions for these species, e.g., the addition of iron minerals for enhancing the potential DIET of *Methanothrix* and biogas productivity (Feng et al., 2010). Furthermore, metaproteomics data could be used to approve/improve metabolic networks (Walke et al., 2021) by, e.g., constraint-based modeling (Koch et al., 2016) or ADM1 (Parker 2005).

The high dominance of a few MAGs could be advantageous for an efficient process. However, missing redundancy in the community could increase sensitivity to metabolic disturbances (acidification) or phage infections, causing at least a transient loss of essential metabolic functions. In this regard, we also observed increased phage protein abundance in H compared to F (Supplementary Figure 16). Increased phage abundance might indicate a higher microbial turnover by phage-induced cell lysis. The reasons could be the elevated growth or the more challenging living conditions in H, including lower pH values, temperature changes, oxygen stress, or traces of antibiotics from the manure. For lysogenic phages, it is known that such conditions may induce a shift from the lysogenic to the lytic cycle (Cochran et al., 1998).

The increased phage presence may promote fast-growing microorganisms and inhibit slow-growing microorganisms focusing on more complex substrates. Furthermore, detailed characterization of the phage proteins and the associated genes in the contigs and MAGs revealed one complete phage genome (Supplementary Note D and Supplementary Fig. 19). This phage genome harbored genes encoding for antibiotic resistance against chloramphenicol (Fernández et al., 2012). This observation showed that phages promote the exchange of genes within an AD microbial community and could increase the ecological fitness of the organisms. On the downside, this represents how antibiotic-resistance genes from animal husbandry could be introduced to nature and the human nutrient cycle. First, the manure is fed to a biogas plant. Subsequently, the fermenter liquid is spread as fertilizer on fields used for food production. Admittedly, we observed that the abundance of MAG_198 decreased from H to F (ratio$MG_{H/F}$: 98.8, ratio$MP_{H/F}$: only in H). However, since it could form spores (e.g., BGA350_8 × 83SP_D8B0_28, spore coat peptide assembly protein cotJB), its long-term survival in ADs and the environment is possible. In the case of the observed chloramphenicol resistance, we cannot link it back to animal husbandry since chloramphenicol has been forbidden in the European Union since 1994 (European Commission 2014). Potentially, other microbes such as *Streptomyces* (Vining and Stuttard 1995)

may synthesize it, or the resistance protein may promote resistance against other antibiotics.

Since our study indicated that the investigated open H did not improve the cleavage of complex carbohydrates, we have to think about novel approaches to enhance the hydrolysis. Therefore, we could mimic better solutions from nature, such as animal rumens. For example, in contrast to the AD microbiome, cow rumen contains larger amounts of anaerobic fungi, which promote the degradation of complex carbohydrates (Hagen et al., 2021). Thus, treatment of digestate with (an)aerobic fungi could be one opportunity (Dollhofer et al., 2018; Kovács et al., 2022), but this is difficult to implement since the living conditions in AD are not well suited for anaerobic fungi (Vinzelj et al., 2020). Furthermore, some publications even suggest that hydrolysis of complex carbohydrates requires the cooperation of the animal host and its microbiome (Khowala et al., 1992; Scoma et al., 2020), for example, by adding host proteins, adjusting the pH value, or a specialized structure of the gastrointestinal tract.

4.3. Metaproteome-based annual microbiome dynamic

Annual metaproteome-based microbiome analysis revealed a stable microbiome in F but a more dynamic microbiome within H. For example, MAG_90 (genus *Pseudoscardovia*) and MAG_223 (genus *Olsenella_B*) nearly disappeared for some time in H. Furthermore, we observed a positive correlation of MAG_223 (genus *Olsenella_B*) and MAG_119 (genus *Eubacterium_H*) to the feeding with sugar beet and corn-cop mix. Since sugar beet and corn-cop mix were fed together, we could not differentiate the effect of both substrates. However, *Olsenella* and *Eubacterium* were also described in other AD fermentations with sugar beets (Montañés et al., 2014) and thus represent potential microbial indicator taxa for this substrate (Vrieze et al., 2016).

Within the functional profile, we observed larger changes in the abundance of proteins for cellulose and hemicellulose degradation. In particular, for sampling time point F10/H10, we observed a high abundance of cellulose and hemicellulose degradation provided mainly by MAG_69 (species *Herbinix luporum*), suggesting that this time point has a higher degradation efficiency. However, confirmation requires balancing the AD and measuring enzyme activities, which was not the scope of this study. Also, correlation analysis revealed no reason why the abundance of cellulose and hemicellulose degradation decreased. Potential molecular reasons for the decreased abundance of MAG_69 include competition, substrate preferences, phages, or changes in the process parameters.

5. Conclusion

MAG-centric metaproteomics unraveled the function of a plethora of microbial species within the AD process. Surprisingly, the microbial community in H does not aid in the degradation of complex carbohydrates but instead mainly hydrolyses easily digestible substrates. These findings question the application of H for increasing yield and productivity of AD and need to be confirmed by sampling other full-scale plants with separated hydrolysis. However, due to the high stability of the microbiome in F, H is potentially involved in stabilizing the microbiome and thereby increasing process stability. Furthermore, we could show that shifts in the feeding result partially in a higher microbiome dynamic.

Declarations

Institutional Review Board Statement: Not applicable.

Informed Consent Statement: Not applicable.

Data Availability Statement: Proteome data were stored on PRIDE with the accession number: PXD044302 (http://www.ebi.ac.uk/pride/archive/projects/PXD044302)

Metagenome datasets were stored on Ena under the project number PRJEB39821. The reads were stored under the number accessions ERS15898928 through ERS15898933. The assembled metagenome data were stored under the number accession ERS17165236.

Author contributions

- Conceptualization: R.H., P.H., D.B.
- Project administration: D.B.
- Sampling and characterization and process parameters: T.M.
- Experiments metagenomics: J.H.
- Experiments metaproteomics: P.H., R.H.
- Data evaluation: R.H., P.H., J.H., I.M., A.S, T.B.
- Bioinformatics: A.S., D.W., R.H., P. H., K.S., I.S.
- Supervision D.B.
- writing—original draft: P.H., R.H., M.K.
- writing—review, and editing: I.M, A.S., J.H., M.K., G.S., U.R., D.B.

All authors have read and agreed to the published version of the manuscript.

Declaration of Competing Interest

The authors declare that they have no known competing financial interests or personal relationships that could have appeared to influence the work reported in this paper.

Data availability

Data will be made available on request.

Funding

This work was supported by the German Federal Ministry of Food and Agriculture (grants nos. 22404015 and 22404115), German Federal Ministry of Education and Research (de.NBI network. project MetaProtServ. grant no. 031L0103), and FKZ for GeneMining grant no. 22031918.

Supplementary materials

Supplementary material associated with this article can be found, in the online version, at doi:10.1016/j.watres.2023.121020.

Supplementary

Supplementary Note
Supplement Table 1 Process Parameters
Supplementary Table 2 *t*-test for dependent samples of process parameters
Supplementary Table 3 Identifications Raw
Supplementary Table 4 Function and taxonomy of identified MAGs
Supplementary Table 5 Protein Identifications
Supplementary Table 6 Calculation Richness and Evenness
Supplementary Table 7 MG and MP Comparison of Metabolic Pathways
Supplementary Table 8 CAZy analysis
Supplementary Table 9 Non-Metabolic Differences
Supplementary Table 10 MAG Dynamic
Supplementary Table 11 Functional_Dynamic
Supplementary Table 12 Correlations
Supplementary Table 13 Phage proteins
Accessions bin sample sheet

References

Abendroth, Christian, Simeonov, Claudia, Peretó, Juli, Antúnez, Oreto, Gavidia, Raquel, Luschnig, Olaf, Porcar, Manuel, 2017. From grass to gas: microbiome dynamics of grass biomass acidification under mesophilic and thermophilic temperatures. Biotechnol. Biofuels 10, 171. https://doi.org/10.1186/s13068-017-0859-0.

Bowers, Robert M., Kyrpides, Nikos C., Stepanauskas, Ramunas, Harmon-Smith, Miranda, Doud, Devin, Reddy, T.B.K., et al., 2017. Minimum information about a single amplified genome (MISAG) and a metagenome-assembled genome (MIMAG) of bacteria and archaea. Nat. Biotechnol. 35 (8), 725–731. https://doi.org/10.1038/nbt.3893.

Buchfink, Benjamin, Xie, Chao, Huson, Daniel H, 2015. Fast and sensitive protein alignment using DIAMOND. Nat. Methods 12 (1), 59–60. https://doi.org/10.1038/nmeth.3176.

Campanaro, Stefano, Treu, Laura, Rodriguez-R, Luis M., Kovalovszki, Adam, Ziels, Ryan M., Maus, Irena, et al., 2020. New insights from the biogas microbiome by comprehensive genome-resolved metagenomics of nearly 1600 species originating from multiple anaerobic digesters. Biotechnol. Biofuels 13, 25. https://doi.org/10.1186/s13068-020-01679-y.

Chaumeil, Pierre-Alain, Mussig, Aaron J., Hugenholtz, Philip, Parks, Donovan H, 2019. GTDB-Tk: a toolkit to classify genomes with the Genome Taxonomy Database. Bioinformatics 36 (6), 1925–1927. https://doi.org/10.1093/bioinformatics/btz848.

Cheng Zhang, Tian, Noike, Tatsuya, 1991. Comparison of One-Phase and Two-Phase Anaerobic Digestion Processes in Characteristics of Substrate Degradation and Bacterial Population Levels. Water Sci. Technol. 23 (7-9), 1157–1166. https://doi.org/10.2166/wst.1991.0567.

Cochran, P.K., Kellogg, C.A., Paul, J.H., 1998. Prophage induction of indigenous marine lysogenic bacteria by environmental pollutants. Mar. Ecol. Prog. Ser. 164, 125–133. https://doi.org/10.3354/meps164125.

Cremonez, Paulo André, Teleken, Joel Gustavo, Meier, Weiser, Ricardo, Thompson, Alves, Helton José, 2021. Two-Stage anaerobic digestion in agroindustrial waste treatment: A review. J. Environ. Manage. 281, 111854 https://doi.org/10.1016/j.jenvman.2020.111854.

Dar, R.A., Parmar, M., Dar, E.A., Sani, R.K., Phutela, U.G., 2021. Biomethanation of agricultural residues: Potential, limitations and possible solutions. Renewable Sustainable Energy Rev. 135, 110217 https://doi.org/10.1016/j.rser.2020.110217.

Dollhofer, Veronika, Dandikas, Vasilis, Dorn-In, Samart, Bauer, Christoph, Lebuhn, Michael, Bauer, Johann, 2018. Accelerated biogas production from lignocellulosic biomass after pre-treatment with Neocallimastix frontalis. Bioresour. Technol. 264, 219–227. https://doi.org/10.1016/j.biortech.2018.05.068.

Drula, Elodie, Garron, Marie-Line, Dogan, Suzan, Lombard, Vincent, Henrissat, Bernard, Terrapon, Nicolas, 2022. The carbohydrate-active enzyme database: functions and literature. Nucleic Acids Res. 50 (D1), D571–D577. https://doi.org/10.1093/nar/gkab1045.

European Commission, 2014. Scientific Opinion on Chloramphenicol in food and feed. EFS2 12 (11). https://doi.org/10.2903/j.efsa.2014.3907.

Feng, Xin Mei, Karlsson, Anna, Svensson, Bo H., Bertilsson, Stefan, 2010. Impact of trace element addition on biogas production from food industrial waste–linking process to microbial communities. FEMS Microbiol. Ecol. 74 (1), 226–240. https://doi.org/10.1111/j.1574-6941.2010.00932.x.

Fernández, Matilde, Conde, Susana, La Torre, Jesús de, Molina-Santiago, Carlos, Ramos, Juan-Luis, Duque, Estrella, 2012. Mechanisms of resistance to chloramphenicol in Pseudomonas putida KT2440. Antimicrob. Agents Chemother. 56 (2), 1001–1009. https://doi.org/10.1128/AAC.05398-11.

Gu, Zuguang, Eils, Roland, Schlesner, Matthias, 2016. Complex heatmaps reveal patterns and correlations in multidimensional genomic data. Bioinformatics 32 (18), 2847–2849. https://doi.org/10.1093/bioinformatics/btw313.

Hagen, Live H., Brooke, Charles G., Shaw, Claire A., Norbeck, Angela D., Piao, Hailan, Arntzen, Magnus Ø., et al., 2021. Proteome specialization of anaerobic fungi during ruminal degradation of recalcitrant plant fiber. ISME J. 15 (2), 421–434. https://doi.org/10.1038/s41396-020-00769-x.

Hassa, Julia, Maus, Irena, Off, Sandra, Pühler, Alfred, Scherer, Paul, Klocke, Michael, Schlüter, Andreas, 2018. Metagenome, metatranscriptome, and metaproteome approaches unraveled compositions and functional relationships of microbial communities residing in biogas plants. Appl. Microbiol. Biotechnol. 102 (12), 5045–5063. https://doi.org/10.1007/s00253-018-8976-7.

Heyer, R., Schallert, K., Siewert, C., Kohrs, F., Greve, J., Maus, I., et al., 2019a. Metaproteome analysis reveals that syntrophy, competition, and phage-host interaction shape microbial communities in biogas plants. Microbiome 7 (1), 69. https://doi.org/10.1186/s40168-019-0673-y.

Heyer, Robert, Schallert, Kay, Büdel, Anja, Zoun, Roman, Dorl, Sebastian, Behne, Alexander, et al., 2019b. A Robust and Universal Metaproteomics Workflow for Research Studies and Routine Diagnostics Within 24 h Using Phenol Extraction, FASP Digest, and the MetaProteomeAnalyzer. Front. Microbiol. 10, 1883. https://doi.org/10.3389/fmicb.2019.01883.

Kang, Dongwan D., Li, Feng, Kirton, Edward, Thomas, Ashleigh, Egan, Rob, An, Hong, Wang, Zhong, 2019. MetaBAT 2: an adaptive binning algorithm for robust and efficient genome reconstruction from metagenome assemblies. PeerJ 7, e7359. https://doi.org/10.7717/peerj.7359.

Khowala, Suman, Ghosh, AnilKumar, Sengupta, Subhabrata, 1992. Saccharification of xylan by an amyloglucosidase of Termitomyces clypeatus and synergism in the presence of xylanase. Appl. Microbiol. Biotechnol. 37 (3), 287–292. https://doi.org/10.1007/BF00210979.

Koch, Sabine, Benndorf, Dirk, Fronk, Karen, Reichl, Udo, Klamt, Steffen, 2016. Predicting compositions of microbial communities from stoichiometric models with applications for the biogas process. Biotechnol. Biofuels 9, 17. https://doi.org/10.1186/s13068-016-0429-x.

Kovács, Etelka, Szűcs, Csilla, Farkas, Attila, Szuhaj, Márk, Maróti, Gergely, Bagi, Zoltán, et al., 2022. Pretreatment of lignocellulosic biogas substrates by filamentous fungi. J. Biotechnol. 360, 160–170. https://doi.org/10.1016/j.jbiotec.2022.10.013.

Lindner, Jonas, Zielonka, Simon, Oechsner, Hans, Lemmer, Andreas, 2016. Is the continuous two-stage anaerobic digestion process well suited for all substrates? Bioresour. Technol. 200, 470–476. https://doi.org/10.1016/j.biortech.2015.10.052.

Ling, Zhenmin, Thakur, Nandini, El-Dalatony, Marwa M., Salama, El-Sayed, Li, Xiangkai, 2022. Protein biomethanation: insight into the microbial nexus. Trends Microbiol. 30 (1), 69–78. https://doi.org/10.1016/j.tim.2021.06.004.

Maus, Irena, Bremges, Andreas, Stolze, Yvonne, Hahnke, Sarah, Cibis, Katharina G., Koeck, Daniela E., et al., 2017. Genomics and prevalence of bacterial and archaeal isolates from biogas-producing microbiomes. Biotechnol. Biofuels 10, 264. https://doi.org/10.1186/s13068-017-0947-1.

Maus, Irena, Klocke, Michael, Derenkó, Jaqueline, Stolze, Yvonne, Beckstette, Michael, Jost, Carsten, et al., 2020a. Impact of process temperature and organic loading rate on cellulolytic /hydrolytic biofilm microbiomes during biomethanation of ryegrass silage revealed by genome-centered metagenomics and metatranscriptomics. Environ. Microbiom. 15 (1), 7. https://doi.org/10.1186/s40793-020-00354-x.

Maus, Irena, Koeck, Daniela E., Cibis, Katharina G., Hahnke, Sarah, Kim, Yong S., Langer, Thomas, et al., 2016. Unraveling the microbiome of a thermophilic biogas plant by metagenome and metatranscriptome analysis complemented by characterization of bacterial and archaeal isolates. Biotechnol. Biofuels 9, 171. https://doi.org/10.1186/s13068-016-0581-3.

Maus, Irena, Tubbesing, Tom, Wibberg, Daniel, Heyer, Robert, Hassa, Julia, Tomazetto, Geizecler, et al., 2020b. The Role of Petrimonas mucosa ING2-E5AT in Mesophilic Biogas Reactor Systems as Deduced from Multiomics Analyses. Microorganisms 8 (12). https://doi.org/10.3390/microorganisms8122024.

Menzel, Theresa, Neubauer, Peter, Junne, Stefan, 2020. Role of Microbial Hydrolysis in Anaerobic Digestion. Energies 13 (21), 5555. https://doi.org/10.3390/en13215555.

Montañés, Rocío, Pérez, Montserrat, Solera, Rosario, 2014. Anaerobic mesophilic co-digestion of sewage sludge and sugar beet pulp lixiviation in batch reactors: Effect of pH control. Chem. Eng. J. 255, 492–499. https://doi.org/10.1016/j.cej.2014.06.074.

Pakarinen, O.M., Tähti, H.P., Rintala, J.A., 2009. One-stage H2 and CH4 and two-stage H2+ CH4 production from grass silage and from solid and liquid fractions of NaOH pre-treated grass silage. Biomass Bioenergy 33 (10), 1419–1427. https://doi.org/10.1016/j.biombioe.2009.06.006.

Parker, Wayne J., 2005. Application of the ADM1 model to advanced anaerobic digestion. Bioresour. Technol. 96 (16), 1832–1842. https://doi.org/10.1016/j.biortech.2005.01.022.

Patel, G.B., SPROTT, G.D., FEIN, J.E., 1990. Isolation and Characterization of Methanobacterium espanolae sp. nov., a Mesophilic, Moderately Acidiphilic Methanogen. Int. J. Syst. Bacteriol. 40 (1), 12–18. https://doi.org/10.1099/00207713-40-1-12.

Pohland, F.G., Ghosh, S., 1971. Developments in anaerobic stabilization of organic wastes–the two-phase concept. Environ. Lett. 1 (4), 255–266. https://doi.org/10.1080/00139307109434990.

Schönberg, Mandy, Linke, Bernd, 2012. The influence of the temperature regime on the formation of methane in a two-phase anaerobic digestion process. Eng. Life Sci. 12 (3), 279–286. https://doi.org/10.1002/elsc.201100062.

Schories, Gerhard, Cordes, Christina, Winterberg, Ralf, 2018. Informationen Und Empfehlungen zum Betrieb landwirtschaftlicher Hydrolyse- und Versäuerungsstufen. Effiziente Hydrolyse und Acidogenese: bioprozesstechnische Optimierung zweiphasiger landwirtschaftlicher Biogasanlagen. Available online at. https://www.bioprozesse.de/wp-content/uploads/2016/05/aceta_brochure_190115_print.pdf.

Scoma, Alberto, Khor, Way Cern, Coma, Marta, Heyer, Robert, Props, Ruben, Schoelynck, Jonas, et al., 2020. Substrate-Dependent Fermentation of Bamboo in Giant Panda Gut Microbiomes: Leaf Primarily to Ethanol and Pith to Lactate. Front. Microbiol. 11, 530. https://doi.org/10.3389/fmicb.2020.00530.

Shen, Fei, Yuan, Hairong, Pang, Yunzhi, Chen, Shulin, Zhu, Baoning, Zou, Dexun, et al., 2013. Performances of anaerobic co-digestion of fruit & vegetable waste (FVW) and food waste (FW): single-phase vs. two-phase. Bioresour. Technol. 144, 80–85. https://doi.org/10.1016/j.biortech.2013.06.099.

Shimada, T., Morgenroth, E., Tandukar, M., Pavlostathis, S.G., Smith, A., Raskin, L., Kilian, R.E., 2011. Syntrophic acetate oxidation in two-phase (acid-methane) anaerobic digesters. Water Sci. Technol. 64 (9), 1812–1820. https://doi.org/10.2166/wst.2011.748.

Sikora, Anna, Detman, Anna, Mielecki, Damian, Chojnacka, Aleksandra, Błaszczyk, Mieczysław (2019): Searching for Metabolic Pathways of Anaerobic Digestion: A Useful List of the Key Enzymes. In J. Rajesh Banu (Ed.): Anaerobic Digestion. Erscheinungsort nicht ermittelbar: IntechOpen.

Stams Alfons, J.M., Teusink, Bas, Sousa Diana, Z., 2019. Ecophysiology of Acetoclastic Methanogens. Eds.. In: Alfons, J.M., Stams Diana, Z.Sousa (Eds.), Biogenesis of Hydrocarbons. Springer International Publishing, Cham, pp. 109–121.

Stolze, Yvonne, Zakrzewski, Martha, Maus, Irena, Eikmeyer, Felix, Jaenicke, Sebastian, Rottmann, Nils, et al., 2015. Comparative metagenomics of biogas-producing microbial communities from production-scale biogas plants operating under wet or dry fermentation conditions. Biotechnol. Biofuels 8, 14. https://doi.org/10.1186/s13068-014-0193-8.

Ubando, Aristotle T., Felix, Charles B., Chen, Wei-Hsin, 2020. Biorefineries in circular bioeconomy: A comprehensive review. Bioresour. Technol. 299, 122585 https://doi.org/10.1016/j.biortech.2019.122585.

Vining, L.C., Stuttard, C., 1995. Chloramphenicol. In Biotechnology. (Reading, Mass) 28, 505–530. https://doi.org/10.1016/B978-0-7506-9095-9.50028-9.

Vinzelj, Julia, Joshi, Akshay, Insam, Heribert, Podmirseg, Sabine Marie, 2020. Employing anaerobic fungi in biogas production: challenges & opportunities. Bioresour. Technol. 300, 122687 https://doi.org/10.1016/j.biortech.2019.122687.

Vrieze, Jo de, Hennebel, Tom, Boon, Nico, Verstraete, Willy, 2012. Methanosarcina: the rediscovered methanogen for heavy duty biomethanation. Bioresour. Technol. 112, 1–9. https://doi.org/10.1016/j.biortech.2012.02.079.

Vrieze, Jo de, Raport, Linde, Roume, Hugo, Vilchez-Vargas, Ramiro, Jáuregui, Ruy, Pieper, Dietmar H., Boon, Nico, 2016. The full-scale anaerobic digestion microbiome is represented by specific marker populations. Water Res. 104, 101–110. https://doi.org/10.1016/j.watres.2016.08.008.

Walke, Daniel, Schallert, Kay, Ramesh, Prasanna, Benndorf, Dirk, Lange, Emanuel, Reichl, Udo, Heyer, Robert, 2021. MPA_Pathway_Tool: User-Friendly, Automatic Assignment of Microbial Community Data on Metabolic Pathways. Int. J. Mol. Sci. 22 (20) https://doi.org/10.3390/ijms222010992.